An Obligate Role for Membrane-Associated Neutral Sphingomyelinase Activity in Orienting Chemotactic Migration of Human Neutrophils

Robert G. Sitrin[1], Timothy M. Sassanella[1], and Howard R. Petty[2]

[1]Division of Pulmonary and Critical Care Medicine, Department of Internal Medicine, and [2]Department of Ophthalmology and Department of Microbiology/Immunology, University of Michigan, Ann Arbor, Michigan

For polymorphonuclear neutrophils (PMNs) to orient migration to chemotactic gradients, weak external asymmetries must be amplified into larger internal signaling gradients. Lipid mediators, associated with the plasma membrane and within the cell, participate in generating these gradients. This study examined the role in PMN chemotaxis of neutral sphingomyelinase (N-SMase), a plasma membrane–associated enzyme that converts sphingomyelin to ceramide. A noncompetitive N-SMase inhibitor, GW4869 (5 mM, 5 minutes), did not inhibit PMN motility (as percentage of motile cells, or mean cell velocity), but it abrogated any orientation of movement toward the source of the chemotaxin, formylmethionylleucylphenylanaline (FMLP) (net displacement along the gradient axis in micrometers, or as percentage of total migration distance). This defect could be completely reversed by treatment with lignoceric ceramide (5 μg/ml, 15 minutes). Immunolocalization studies demonstrated that N-SMase (*1*) distributes preferentially toward the leading edge of some elongated cells, (*2*) is associated with the plasma membrane, (*3*) is more than 99.5% localized to the cytofacial aspect of the plasma membrane, (*4*) is excluded from pseudopodial extensions, and (*5*) increases rapidly in response to FMLP. Morphologically, the inhibition of N-SMase limited cellular spreading and the extension of sheet-like pseudopods. Elongated PMNs demonstrated a polarized distribution of GTPases, with Rac 1/2 accumulated at, and RhoA excluded from, the front of the cell. This polarity was negated by N-SMase inhibition and restored by lignoceric ceramide. We conclude that N-SMase at the cytofacial plasma membrane is an essential element for the proper orientation of PMNs in FMLP gradients, at least in part by polarizing the distribution of Rac 1/2 and RhoA GTPases.

Keywords: neutrophil; chemotaxis; sphingomyelinase; ceramide; sphingolipid

Polymorphonuclear neutrophils (PMNs) accumulate at inflammatory foci because they are capable of recognizing and migrating toward chemotactic signals. For PMNs to polarize their morphology and orient their movement to chemotactic gradients, complex spatial redistributions of membrane constituents, downstream signaling molecules, and cytoskeletal structures must occur (1–4). Although the distribution of surface receptors and intracellular signaling proteins has been the primary focus of attention, recent evidence highlighted the importance of highly compartmentalized membrane lipids and lipid-signaling molecules (1, 3, 4). In part, this compartmentalization may be achieved by a polarized distribution of sphingolipid-enriched microdomains within the plasma membrane (1, 5, 6). Although the diffusion of mobile lipids and the reorganization of stable sphingolipid-enriched microdomains could contribute to a structural and functional polarization of the plasma membrane, we hypothesized that lipid-modifying enzymes could also regulate lipid-mediated signaling. Here, we focused on the function of neutral sphingomyelinase, which hydrolyzes sphingomyelin in the plasma membrane to ceramide. Ceramide, the core structure of complex sphingolipids, is composed of varying fatty acids (predominately 16–24 carbon atoms), linked to a sphingoid base (7). It has drawn particular interest as an intracellular signaling molecule because it regulates multiple pathways, including those of protein phosphatases PP1 and PP2A, protein kinase Cζ, phospholipase D, Ca^{2+} influx, mitogen-activated protein kinase, and c-jun N-terminal kinase (8, 9). Ceramide can also activate mononuclear phagocytes by binding to CD14, resulting in downstream signaling events that overlap with those triggered by lipopolysaccharide (10, 11). It exerts both excitatory and inhibitory effects on a wide array of complex effector functions, including phagocytosis, degranulation, oxidant generation, integrin-mediated adhesion, and apoptosis (8, 12–16). Although ceramide clearly acts at some intracellular sites, other signaling properties likely relate to its function in the plasma membrane. Its structure favors extensive hydrogen bonding between head groups, facilitating homotypic aggregation into ceramide-rich patches (7). These patches have the potential to induce regional heterogeneities in signaling events, membrane rigidity, physical curvature, lipid packing, conformation of membrane-associated proteins, and solute efflux (7, 9, 17). Further, ceramide appears to be necessary for capping (and the capping-induced signaling) of certain receptors, including L-selectin and Fas (7). Ceramide generation, a common response to many external stresses, can occur slowly by *de novo* synthesis in the endoplasmic reticulum/Golgi complex, or rapidly by hydrolysis of sphingomyelin, a normal constituent of PMN plasma membranes (9). Sphingomyelinases, expressed in all cell types, are generally categorized as acidic (lysosomal) versus membrane-associated, Mg^{2+}-dependent neutral sphingomyelinase (N-SMase; optimal pH, 7.4). Ninety-nine percent of human PMN SMase activity is attributed to N-SMase (in the N-SMase2 isoform), and is largely associated with the plasma membrane (16, 18). N-SMase was implicated in many

CLINICAL RELEVANCE

We describe a novel mechanism for the regulation of neutrophil chemotaxis. The identification of new therapeutic targets for regulating acute inflammation would have broad implications for the management of inflammatory lung diseases, including pneumonia, sepsis syndrome, and acute respiratory distress syndrome.

(*Received in original form January 11, 2010 and in final form March 29, 2010*)

This work was supported by National Institutes of Health grants RO1 AI060983 (R.G.S.) and CA74120 (H.R.P.).

Correspondence and requests for reprints should be addressed to Robert G. Sitrin, M.D., Division of Pulmonary and Critical Care Medicine, Department of Internal Medicine, University of Michigan, 1150 West Medical Center Dr., 6301 MSRB III, SPC 5642, Ann Arbor, MI 48109-5642. E-mail: rsitrin@umich.edu

Am J Respir Cell Mol Biol Vol 44. pp 205–212, 2011
Originally Published in Press as DOI: 10.1165/rcmb.2010-0019OC on April 8, 2010
Internet address: www.atsjournals.org

PMN functions, including phagocytosis, oxidant generation, and apoptosis (16, 19). Membrane-associated N-SMase activity doubles with formylmethionylleucylphenylalanine (FMLP) stimulation, but its involvement in PMN chemotaxis has not been investigated (16). Here, we demonstrate that N-SMase activity associated with the plasma membrane is critical for PMN to orient migration to a chemotactic gradient of FMLP.

MATERIALS AND METHODS

PMN Purification

PMNs were isolated from peripheral blood obtained from healthy volunteers in compliance with the Institutional Review Board for Human Subject Research at the University of Michigan. Briefly, citrate-anticoagulated blood was sedimented with 6% dextran/0.9% NaCl. Erythrocytes were removed by hypotonic lysis, and PMNs were isolated to more than 95% purity by density gradient centrifugation on 10% Ficoll-Hypaque.

Analysis of Chemotaxis by Single-Cell Tracking

PMNs were adhered to coverslips and pretreated with GW4869, a noncompetitive N-SMase inhibitor (5 μM, 5 minutes; Calbiochem, San Diego, CA), or Hanks' balanced salt solution (HBSS). The coverslips were then applied to Dunn chemotaxis chambers (Hawksley, Lancing, Sussex, UK). The outer rings of the chambers were loaded with FMLP (5×10^{-7} M in HBSS; Sigma, St. Louis, MO) to establish chemotactic gradients. Serial images of a field of cells maintained at 37°C were then collected at 30-second intervals for 30 minutes. Cell coordinates were plotted manually at each frame, and the image stacks were processed with Metamorph 7.1.2.0 software (Molecular Devices, Downingtown, PA) and Microsoft Excel (Microsoft, Redmond, WA) to analyze the movements of individual cells. A pixel-to-micrometer conversion was established by imaging a calibration slide under identical conditions. A PMN was considered motile if it moved at least 30 μm from its original coordinates at any point during the observation period, proportionate to a threshold used previously for shorter viewing periods (20). Among motile cells, the mean cell velocity (μm/minute) was calculated from the total distance traveled over 30 minutes. To assess the directional bias of movement, the net displacement along the axis of the gradient over 30 minutes was measured (in micrometers), and also expressed as a chemotactic index, calculated as the displacement along the gradient as a percentage of the total path distance (21). For pooled data, each data point represents the mean values obtained from at least 60 cell tracks in each experiment, and n represents the number of independent experiments, each with a unique donor.

To examine the effects of exogenous sphingolipids, PMNs were pretreated for 15 minutes at 37°C with (*1*) lignoceric ($C_{24:0}$) ceramide (5 μg/ml; Cayman Chemicals, Ann Arbor, MI) diluted in 0.5% DMSO/HBSS, or (*2*) sphingomyelin (5 μg/ml; Enzo Life Sciences, Plymouth Meeting, PA) in 0.5% DMSO/HBSS for 15 minutes. When ceramide was used to rescue the effects of GW4869, the two pretreatments were performed successively, with GW4869 followed by ceramide.

Immunolabeling

Mouse anti-Rac1/2 (clone 23A8; Upstate Biotech/Millipore, Billerica, MA) and mouse anti-RhoA (Cytoskeleton, Inc., Denver, CO) were conjugated with Alexa Fluor 555 (Invitrogen, Carlsbad, CA). Goat anti-human N-SMase2 antibody (Ab) (Santa Cruz Biotechnology, Santa Cruz, CA) was conjugated to Alexa Fluor 546 (Invitrogen). All conjugation steps were performed with a FluoReporter Protein Labeling Kit (Invitrogen). PMNs were adhered to MatTek dishes (MatTek Corp., Ashland, MA) and stimulated with FMLP (5×10^{-7}M in HBSS) for 30 minutes at 37°C in 5% CO_2. Cells were then fixed with 25% glutaraldehyde in HBSS for 20 minutes, washed with HBSS, permeabilized with 0.01% saponin for 10 minutes, blocked with 10% serum, incubated with labeled Ab for 30 minutes at room temperature, and washed with HBSS/1% BSA. Nuclei were counterstained with Hoechst 33342 (Invitrogen). Cells were imaged immediately after immunostaining, using a Nikon Eclipse TE-2000U microscope (Nikon Instruments, Melville, NY). For confocal microscopy, images were taken using an Olympus IX-71 inverted microscope, (Olympus, Center Valley, PA) using laser excitation at 488 nm and 543 nm, and fitted with Olympus FluoView 500 laser scanning confocal accessories.

Scanning Electron Microscopy

PMNs were treated as indicated and fixed with 2.5% glutaraldehyde in Sorenson's buffer, pH 7.4, followed by 1.0% OSO_4, freeze-fractured in liquid N_2, and dehydrated with stepwise immersion in 30% to 100% ethanol. Cells were then immersed in hexamethyldisilazane, mounted in colloidal graphite and Duco cement, and sputter-coated with gold. Scanning electron microscopy was performed by the University of Michigan Microscopy Image Analysis Laboratory with an AMRAY 1910 Field Emission Scanning Electron Microscope KLA-Tencor (Milpitas, CA), and digital image acquisition using a SEMICAPS Inc. (Dallas, TX) digital interface.

Flow Cytometry

Goat anti-human N-SMase Ab (Santa Cruz Biotechnology) was labeled with Oregon Green 488 (Invitrogen), using a FluoReporter Protein Labeling Kit. After pretreatments as indicated, PMNs were blocked with 1% goat serum for 5 minutes on ice, incubated with 1 ng/ml labeled Ab for 20 minutes, and washed to measure N-SMase on the cell exterior. Then aliquots of cells were treated with anti-Oregon Green goat IgG (Invitrogen) on ice for 20 minutes, to quench any anti-N-SMase Ab bound to the cell exterior. Cells were fixed with iced 4% formalin in HBSS, pH 7.4, for 15 minutes, pelleted, and resuspended in HBSS, so that the quenched anti-N-SMase Ab was fixed on the cell exterior. To measure intracellular N-SMase, fixed cells were permeabilized with 0.01% saponin for 10 minutes, blocked with 1% goat serum for 20 minutes, relabeled with 1 ng/ml Oregon Green 488/anti N-SMase Ab for 20 minutes, and washed. Mean fluorescence intensities (linear scale) were determined from at least 10,000 cells as a measure of relative antigen expression, using an EPICS Elite ESP flow cytometer (Coulter, Miami FL) at the University of Michigan Flow Cytometry Core Facility.

Statistical Analyses

Group means were compared with the Student t test, and multiple comparisons were performed using one-way ANOVA. We used χ^2 analyses for contingency tables. All analyses were performed with GraphPad Prism, version 5.00 for Windows (GraphPad Software, San Diego, CA).

RESULTS

Effects of N-SMase Inhibition on PMN Chemotaxis

In the first series of experiments, PMNs were pretreated with GW4869 (5 μM, for 5 minutes, at 37°C), a highly specific noncompetitive inhibitor of N-SMase (22), and loaded into Dunn chemotaxis chambers charged with FMLP (5×10^{-7} M). Compared with diluent-pretreated controls, GW4869 had no effect on the percentage of motile cells, whereas mean cell velocity increased slightly ($P < 0.05$), indicating that N-SMase inhibition was neither toxic to the cells nor able to impede cell locomotion (Figures 1A and 1B). By contrast, GW4869 completely negated the directional bias of migration toward the FMLP source, as determined by the mean net displacement along the gradient axis and the chemotactic index (both $P < 0.0001$; Figures 1C and 1D; $n = 12$, ≥ 60 tracks per experiment). In fact, the mean displacement of GW4869-treated cells was directed significantly away from the FMLP source ($P < 0.05$). To highlight the behavior of individual cells, a compilation of displacements along the axis of the chemotactic gradient (D_{axis}) data is shown as a scatterplot, including almost 1,000 tracks from the 12 donors, along with corresponding histograms (Figures 1E and F). The D_{axis} of both control samples and GW4869-treated cells distributed broadly, with most cells in both groups achieving little net movement along the gradient. Nonetheless, a Kruskal–Wallis test applied to a one-way ANOVA demonstrated that the net displacements under the

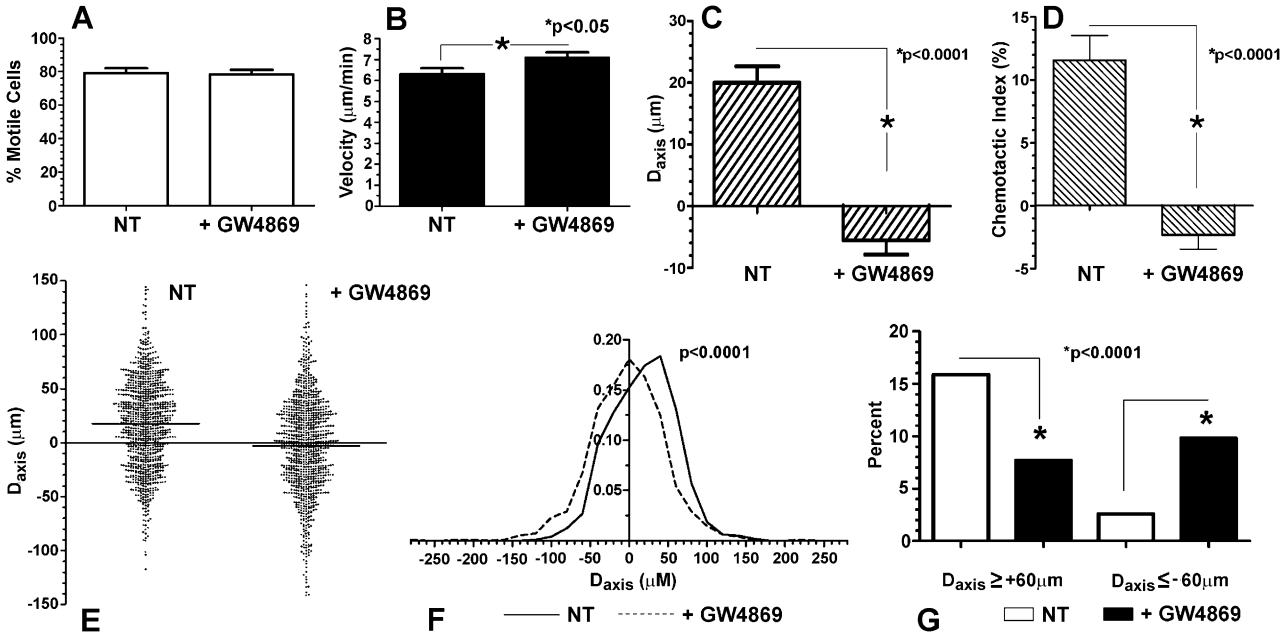

Figure 1. Effects of inhibiting neutral sphingomyelinase (N-SMase) on formylmethionylleucylphenylalanine (FMLP) induced PMN chemotaxis. PMNs pretreated with buffer (*NT*) or GW4869 (5 mM) were loaded onto Dunn chambers charged with FMLP (5×10^{-7}M), and cell tracks were assembled from serial images over 30 minutes. GW4869 did not significantly affect the percentage of motile cells (*A*), and it slightly increased mean cell velocity (*B*). (*C*) However, the net displacement along the axis of the chemotactic gradient was negated, with net movement directed away from the FMLP source ($P < 0.05$). (*D*) Accordingly, the chemotactic index (displacement along the gradient axis as percentage of total path length) was reduced to near-zero (mean ± SEM, $n = 12$, ⩾ 60 cell tracks per experiment). The effects of N-SMase inhibition on the net displacement of individual PMNs migrating in FMLP gradients are shown in scatterplots (*E*) (three off-scale tracks in each group are not shown) and histograms (*F*), using the same pool of cells as in *A–D*. GW4869 negated the group progress toward the FMLP source (Kruskal–Wallis *post hoc* test applied to one-way ANOVA, $P < 0.0001$). (*G*) A frequency analysis (χ^2) of the number of cell tracks displaced at least 60 μm toward or away from the FMLP source (data are shown as percentages of total cell tracks).

two conditions were significantly different ($P < 0.0001$). To focus on cells with the greatest directional migration, the D_{axis} was at least 60 μm in 154/969 cells (15.9%) of the control samples, versus 74/962 (7.7%) of GW4689-treated cells (Figure 1G; $P < 0.0001$, χ^2 analysis). By contrast, 94/962 (9.8%) of the GW4869-treated cells moved at least 60 μm in the opposite direction from the FMLP source, versus only 25/969 (2.6%) of control cells ($P < 0.0001$).

Because N-SMase converts sphingomyelin to ceramide, the two most immediate effects to account for the loss of directional migration would involve the loss of a critical pool of ceramide, or an accumulation of sphingomyelin. However, a nonspecific effect of GW4869, unrelated to N-SMase inhibition, could not be excluded. To address these issues, PMNs were successively treated with GW4869 and lignoceric ceramide (5 μg/ml, for 15 minutes at 37°C) or diluent control. As shown in Figure 2, exogenous ceramide completely rescued directionally biased migration toward the FMLP source, while leaving both the percentage of motile cells and mean cell velocity unaffected. To determine whether ceramide alone affects chemotaxis or else specifically rescues the defect created by GW4869, PMNs were pretreated with ceramide or diluent control without GW4869, and then exposed to the FMLP gradient. As shown in Figures 3A−3D, ceramide alone had no effect on chemotaxis, further reinforcing the specificity of GW4869 as an inhibitor of N-SMase. To address the possibility that an accumulation of

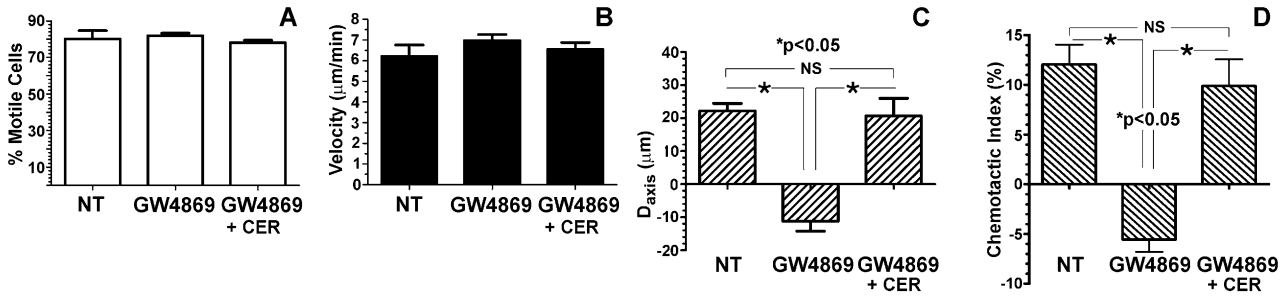

Figure 2. Exogenous ceramide (*CER*) reverses the effects of N-SMase inhibition on FMLP-induced PMN chemotaxis. PMNs were pretreated with buffer, GW4869 (5 mM), or GW4869 with lignoceric ceramide (5 μg/ml), as described in Materials and Methods. PMNs were then loaded onto Dunn chambers charged with FMLP (5×10^{-7} M). Data are expressed as in Figure 1. Exogenous ceramide completely restored the mean displacement along the FMLP gradient (*C*) and the chemotactic index (*D*) to levels equivalent to control cells, reversing the inhibitory effects of GW4869. *P* values refer to the results of Bonferroni *post hoc* tests applied to one-way ANOVA. Values are given as mean ± SEM ($n = 5$, ⩾ 60 cell tracks per experiment).

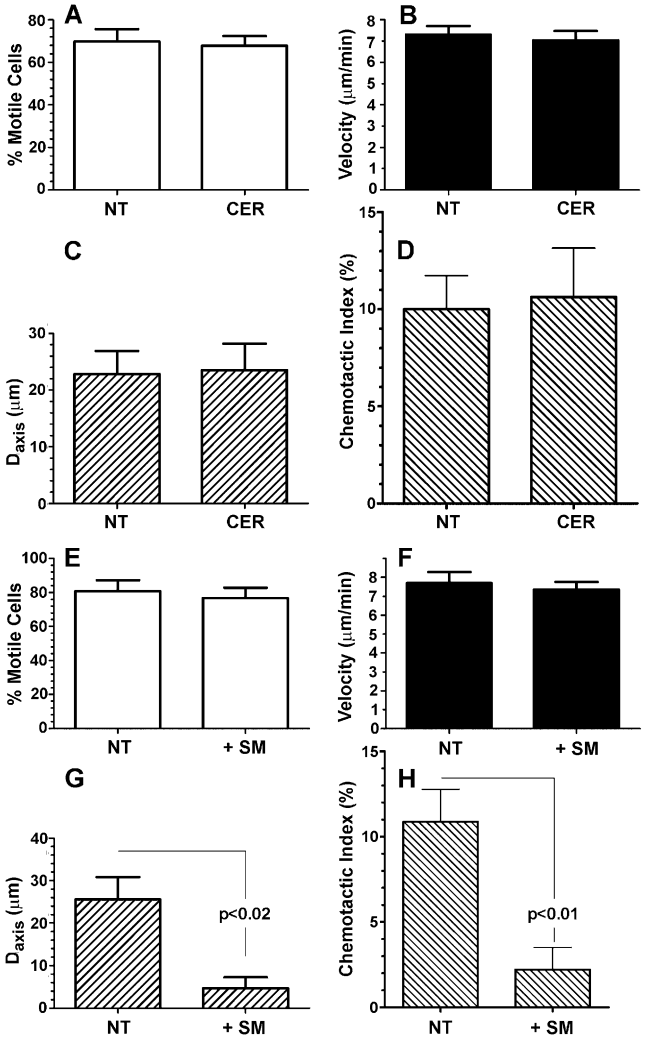

Figure 3. Effects of exogenous ceramide and sphingomyelin (SM) on FMLP-induced chemotaxis. (*A–D*) Exogenous ceramide (5 μg/ml) had no effects on motility, displacement along the gradient, or chemotactic index, relative to untreated control samples. Exogenous sphingomyelin (5 μg/ml) did not affect the percentage of motile cells (*E*) or cell velocity (*F*), but partly suppressed displacement along the axis of the FMLP gradient (D_{axis}) (*G*) ($P < 0.02$) and the chemotactic index (*H*) ($P < 0.01$) ($n = 4$). Data are expressed as in Figure 1 ($n = 6$, ≥ 60 cell tracks per experiment).

sphingomyelin could duplicate the effects of GW4869, PMNs were pretreated with sphingomyelin (5 μg/ml, for 15 minutes at 37°C) or diluent, and exposed to FMLP gradients in a fashion identical to that in the previous experiments. As shown in Figures 3E–3H, exogenous sphingomyelin had no effect on percent motility or velocity, but decreased the D_{axis} and chemotactic index. As a control, PMNs were instead treated with $C_{24:0}$ phosphatidylcholine (5 μg/ml, for 15 minutes at 37°C; Avanti Polar Lipids, Inc., Alabaster AL), which had no effect at all on motility or directional migration (data not shown). Thus, the accumulation of sphingomyelin could have contributed to the effects of GW4869, although it was not nearly as effective. Further, the ability of ceramide to reverse the effects of GW4869 completely suggests that a loss of ceramide production is the dominant mechanism by which N-SMase inhibition negates directionally biased migration. Neither ceramide nor sphingomyelin affected spontaneous migration in the absence of an FMLP gradient (not shown).

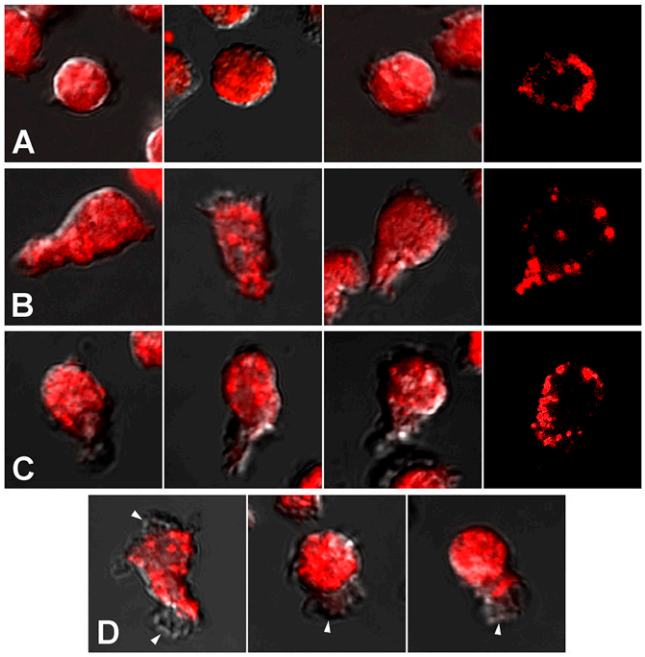

Figure 4. Subcellular localization of N-SMase. PMNs were stimulated with FMLP (5×10^{-7} M), fixed, permeabilized, and immunolabeled, as described in Materials and Methods. Images of N-SMase immunofluorescence were merged with differential interference contrast microscopy images to highlight cell outlines. (*A*) N-SMase was distributed uniformly in round PMNs. Some elongated PMNs (*B*) demonstrated no front-to-back asymmetry in the distribution of N-SMase, whereas others (*C*) demonstrated preferential expression toward the front of the cell, and little at the tail. Confocal images in each row (*far right*) demonstrate that immunostaining was associated with the plasma membrane, with virtually no immunostaining in the cell interior. (*D*) N-SMase was virtually excluded from any pseudopodial extensions (arrows) anywhere on the cells.

Immunolocalization of N-SMase

PMNs were treated with a uniform concentration of FMLP (5×10^{-7} M, 15 minutes), fixed, permeabilized, stained with Alexa Fluor 456–labeled anti–N-SMase Ab, and imaged by fluorescence microscopy and differential interference contrast microscopy. As shown in Figure 4, the distribution of N-SMase is relatively uniform throughout the bodies of round PMNs. The N-SMase on some elongated PMNs was uniformly distributed, whereas in others, a notable accumulation occurred toward the front of the cell, with relatively weak expression at the tail. Confocal images indicate that N-SMase is associated with the plasma membrane, rather than being distributed diffusely in the cytoplasm. Further, the merged images indicate that pseudopodial extensions at the leading edges and elsewhere are virtually devoid of N-SMase immunoreactivity. Lastly, flow cytometry was used to determine the extent to which N-SMase distributes asymmetrically to the exofacial versus cytofacial aspect of the plasma membrane. N-SMase was virtually undetectable on the cell exterior (0.4% of total immunoreactivity; Figure 5A). Combined with the confocal images, these findings indicate that the great preponderance of N-SMase activity is associated with the cytofacial leaflet of the plasma membrane, as described previously (23). The distribution of N-SMase in unstimulated cells was indistinguishable in unstimulated versus FMLP-stimulated cells (not shown). However, flow cytometry demonstrated that the total N-SMase in permeabilized cells increased significantly within 15 minutes of FMLP stimulation (Figure 5B). The rapidity

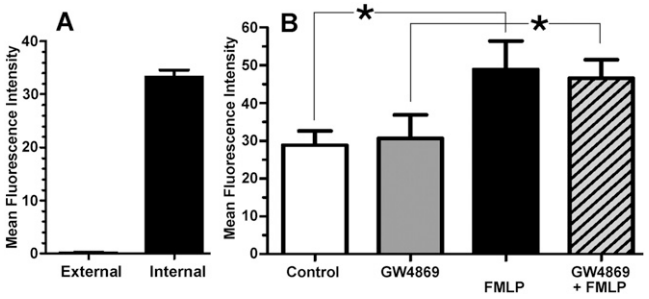

Figure 5. N-SMase expression according to flow cytometry. (*A*) Flow cytometry was performed on fixed/permeabilized PMNs labeled with Oregon Green–conjugated anti-SMase antibody (Ab). Compared with untreated control samples, FMLP (5×10^{-7} M for 15 minutes) significantly increased N-SMase immunoreactivity, whereas GW4869 had no effect, either on untreated or FMLP-treated cells. Data are expressed as mean fluorescence intensity (MFI) of at least 10,000 cells per experiment (mean ± SEM, $n = 4$). (*B*) Flow cytometry was performed on PMNs that were labeled to measure external immunoreactivity. Aliquots of these cells were then treated with anti–Oregon Green 488 Ab to quench external labeling, followed by fixation/permeabilization and relabeling with anti–N-SMase Ab to measure internal N-SMase immunoreactivity, as described in MATERIALS AND METHODS. Data are expressed as MFI of at least 10,000 cells per experiment (mean ± SEM, $n = 4$). External MFI was 0.4% of internal MFI; $^*P < 0.05$.

this effect precludes the possibility of N-SMase neosynthesis, suggesting instead that FMLP induces changes in the conformation or microenvironment of N-SMase that enhance the intensity of its immunolabeling. In keeping with this observation, previous work demonstrated that FMLP stimulation doubles the N-SMase activity associated with plasma membrane fractions *in vitro* (16). GW4869 had no effect on the amount of N-SMase antigen detected in either unstimulated or FMLP-stimulated cells (Figure 5).

Effects of N-SMase Inhibition and Ceramide on PMN Morphology

Scanning electron microscopy was performed to determine if manipulating N-SMase activity exerted effects on PMN morphology that paralleled its effects on chemotaxis. PMNs were stimulated with uniform concentrations of FMLP (10^{-7} M) ± GW4869 and lignoceric ceramide, as described for the cell-tracking experiments, and were then processed for scanning electron microscopy. Representative images are provided in Figure 6. Compared with cells treated with FMLP alone, GW4869 caused elongated PMNs to desist from spreading, partially detach from the surface, and limit pseudopodial extensions to a few narrow spikes. Just as lignoceric ceramide rescued directionally biased migration, it restored the spreading, adhesion, and formation of extended, sheet-like pseudopodia to FMLP/GW4869–treated cells. However, ceramide alone did not affect the morphology of elongated FMLP-stimulated cells. Treatment with sphingomyelin caused partial detachment, and limited pseudopod formation in a fashion similar to that of GW4869, consistent with the similar effects of sphingomyelin on directional migration. The effects on morphology were limited to elongated cells, because GW4869 did not affect the appearance of PMNs that retained a rounded shape in the presence of FMLP (not shown).

Effects of N-SMase on Rac 1/2 and RhoA Distribution

Because N-SMase inhibition selectively inhibits the orientation of PMNs along a chemotactic gradient, we sought to determine

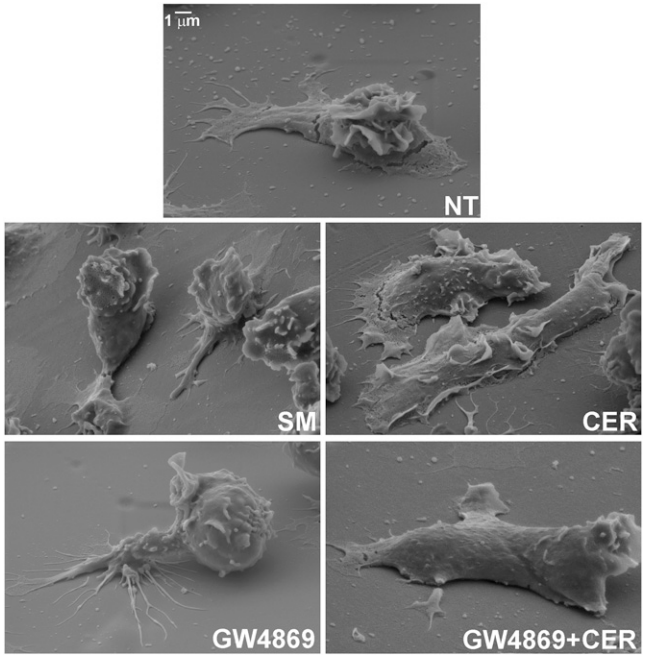

Figure 6. Effects of N-SMase inhibition and ceramide reconstitution on PMN morphology. Scanning electron microscopy was performed on PMNs treated with buffer, GW4869 (5 mM), or GW4869 with lignoceric ceramide (5 μg/ml), as described in MATERIALS AND METHODS, followed by FMLP (5×10^{-7} M). Compared with cells treated with FMLP alone (*NT*), N-SMase inhibition with GW4869 caused elongated PMNs to limit their spreading, partially detach from the surface, and limit pseudopodial extensions to a few narrow spikes. Lignoceric ceramide restored spreading, adhesion, and the formation of extended, sheet-like pseudopodia to FMLP/GW4869–treated cells.

if this inhibition could be caused by a loss of internal asymmetry of the internal signaling molecules known to be integrated in the PMN "compass" system, such as Rac 1/2 and RhoA GTPases. As shown in Figure 7, Rac 1/2 localizes toward the front of the cell, and is weakly expressed toward the tail, whereas N-SMase inhibition leads to a uniform distribution. Treatment with lignoceric ceramide restored localization at the leading edge, just as it restores orientation along a chemotactic gradient. By contrast, RhoA was excluded from the leading edges of elongated cells, but was relatively uniform elsewhere, as described previously (24). N-SMase inhibition with GW4869 caused RhoA to appear at the leading edge, and this was also reversed with lignoceric ceramide. Thus, one function of the ceramide generated by N-SMase is apparently to maintain the proper orientation of these internal signaling gradients.

DISCUSSION

Lipids, either intracellular or within the plasma membrane, engage multiple signaling pathways involved in cellular migration (1, 3, 4). The polarized distribution of membrane sphingolipids is a common characteristic of migrating leukocytes (1, 25). Previous work showed that disrupting sphingolipid-enriched microdomains may slow or immobilize PMNs (20, 26) or selectively interfere with their orientation toward a chemotaxin (27), but important questions remain unanswered regarding whether sphingolipids were responsible, and by what mechanisms they may have functioned. Here, we examined the effects of N-SMase and its proximate product, ceramide, on PMN chemotaxis. High-throughput analyses of large numbers of cell

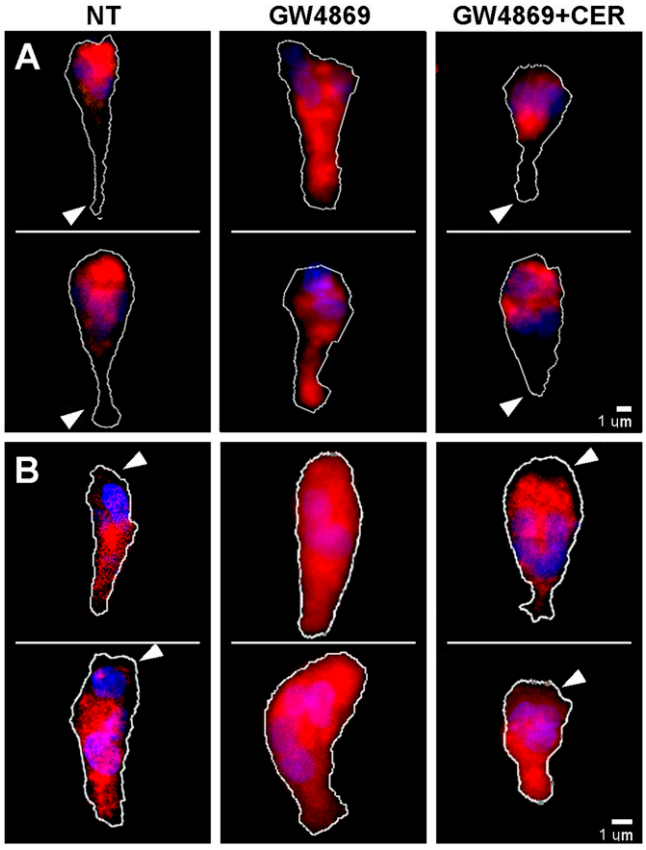

Figure 7. Effects of N-SMase inhibition and lignoceric ceramide on the distribution of Rac 1/2 and RhoA GTPases. Immunofluorescence microscopy of fixed/permeabilized FMLP-treated PMNs was performed as described in MATERIALS AND METHODS. Two cells representative of each treatment condition are shown. (*A*) Rac 1/2 was concentrated at the leading edge of elongated PMNs, with weak expression at the tail (*arrowheads*), whereas GW4869 (5 mM) caused the distribution to be uniform. Lignoceric ceramide (5 μg/ml) added to GW4869-treated cells restored the concentration of Rac 1/2 at the leading edge, with relative exclusion at the tail (*arrowheads*). (*B*) RhoA was excluded from the leading edge in elongated PMN (*arrowheads*). GW4869 (5 mM) caused RhoA to redistribute to the leading edge, rendering a uniform distribution over the cell. Lignoceric ceramide (5 μg/ml) added to GW4869-treated cells restored the exclusion of RhoA from the leading edge (*arrowheads*). *Dotted lines* indicate cell outlines.

tracks permitted us to discriminate between the effects on locomotion versus orientation during movement along FMLP gradients. N-SMase activity was shown to be essential for PMNs to bias their migration toward a FMLP source, whereas it played no role in the intrinsic motility of the cells (percentage of motile cells or mean cell velocity; Figures 1A and 1B). An accumulation of sphingomyelin also caused significant loss of directional bias (Figure 3), but the effect was not as complete as with N-SMase inhibition, and the ability of exogenous ceramide to restore chemotaxis fully after N-SMase inhibition suggests that the responsible agents are predominately ceramide and/or its metabolites. The isolated effect on orientation versus locomotion strongly suggests that N-SMase activity and ceramide are selectively engaged in generating or maintaining signaling polarity. Notably, ceramide did not have to be applied focally to PMNs to exert this effect on polarity, although ceramide may have distributed to specific regions after it was incorporated into the plasma membrane.

The pluripotency of ceramide suggests that multiple mechanisms may be at play, but we can conclude at least that N-SMase and ceramide strongly influence the asymmetrical distribution of Rac 1/2 versus RhoA GTPases (Figure 7), a distribution that was implicated in the front/back polarity of migrating PMNs (26, 28, 29). The complex mechanisms underlying the orientation of PMNs toward a chemotaxin involve a spatial strategy whereby weakly asymmetrical external signals are greatly amplified into steep internal signaling gradients (3, 26, 28, 30). Many of these internal signals involve lipids, including phosphatidylinositol 3,4,5-trisphosphate and phosphatidic acid, which may preferentially associate with sphingolipid-enriched microdomains (1, 4, 26, 31). However, previous studies showed that selectively ablating these pathways does not necessarily disrupt chemotaxis, consistent with the redundant signaling or shared functions of multiple isoforms within a pathway (3, 30). In this context, the effect of N-SMase inhibition was strikingly specific and complete, suggesting that its fundamental role in maintaining function polarity is not easily circumvented by alternative signaling pathways.

Ceramide has an extensive signaling portfolio relevant to chemotaxin responsiveness. Ceramide aggregates, capable of triggering localized Ca^{2+} entry and solute efflux, are necessary for the aggregation and signaling competency of receptors such as L-selectin and Fas (7). Other potentially important effects include the activation of protein phosphatase 2A and calpain, and the inhibition of paxillin phosphorylation, mitogen-activated protein (MAP) kinase, and phospholipase D (8, 14, 16, 32–35). Only limited evidence has implicated ceramide in chemotaxis. Lactosylceramide, an abundant ceramide metabolite, can be loaded into differentiated HL-60 cells to induce migration (36). By contrast, ceramide was shown to modulate many other effector functions, including the production of cytokines and reactive oxygen intermediates, phagocytosis, β2 integrin expression, degranulation, and apoptosis (8, 13, 37–39).

Further work will be necessary to determine the extent to which our findings apply to PMN chemotaxis under other conditions. First, the chemotaxin may be an important variable, because PMN responsiveness was shown to be hierarchical, with signals engaged by "end target" chemotaxins (e.g., FMLP and C5a) overriding those generated by "intermediate" chemotaxins (e.g., IL-8 and leukotriene B4), and proceeding through different signaling mechanisms (3, 40, 41). Second, the characteristics of PMN tracks under the conditions used in this study (frequent directional changes, with a chemotactic index of $\sim$ 10%) are most compatible with a "biased random walk" pattern characteristic of cells in a shallow chemotactic gradient (3). Therefore, whether N-SMase functions similarly in steep gradients, where more linear movement along the gradient axis would be expected, remains to be seen. Lastly, we constructed a two-dimensional system to favor the movements of loosely adherent cells. N-SMase could function differently in the presence of extracellular matrix proteins, or in a three-dimensional system, because of offsetting effects on adhesion and deformability.

Importantly, ceramide is readily metabolized along several pathways to products that pertain to this discussion (42). Ceramidase can convert ceramide to sphingosine, which in turn is phosphorylated to sphingosine-1–phosphate (S1P) by sphingosine kinase. S1P has an established role in cellular migration, binding to a family of receptors (Edg) that stimulate migration in many cell types, including PMNs (43, 44). Sphingosine kinase was also implicated in PMN priming, Ca^{2+} signaling, and migration (45). Lastly, ceramide may be glycosylated by glucosylceramide synthase (GCS) as a first step in synthesizing a large array of glycosphingolipids. Because GCS is usually found in the Golgi complex, this pathway is not likely to be relevant to

the present study, because the effects of exogenous ceramide are too rapid for this processing route (46). Further studies will need to determine how ceramide metabolites are involved in the effects of N-SMase on PMN chemotaxis.

N-SMase was associated with the cytofacial aspect of the plasma membrane (Figures 4 and 5), in agreement with previous work (16, 23). Sphingomyelin in the exofacial plasma membrane could still be the substrate for this N-SMase, because Ca^{2+}-activated scramblase activity or a loss of membrane lipid symmetry at ceramide aggregates could deliver sphingomyelin to the cytofacial membrane. Alternately, sphingomyelin mobilized from the Golgi complex is a plausible source (47, 48). The variable front–back asymmetry of N-SMase localization (Figure 4) suggests that the distribution of N-SMase may be dynamic, rather than a static feature of cell polarity. Nonetheless, functional asymmetries are generated downstream, such as the distributions of Rac 1/2 and RhoA (Figure 7). Another striking aspect of N-SMase localization is its virtual absence from pseudopodial membranes (Figure 5). This feature was not described previously, although it is consistent with the observation that platelet pseudopods are relatively enriched in sphingomyelin (49). At present, we can only speculate that the absence of N-SMase in pseudopodial membranes may occur because N-SMase is constrained by association with membrane proteins or larger domains that are not incorporated into extending pseudopods. However, the absence of N-SMase may hold intriguing functional implications for extending pseudopods. For example, ceramide inhibits phospholipase D activity, and thus the exclusion of N-SMase/ceramide may permit the localized generation of phosphatidic acid, a lipid mediator recently shown to be important in the stable localization of Docking protein 2 and leading edge formation (4, 8).

In conclusion, we demonstrate that N-SMase activity associated with the plasma membrane is necessary for PMNs to develop functional polarity in an FMLP gradient, as manifested by the distribution of Rac 1/2/RhoA GTPases and directionally biased migration. Thus sphingolipids, and ceramide in particular, join the growing list of lipid mediators that mediate the orientation of PMNs under the influence of chemotaxins.

Author Disclosure: R.G.S. has served as an expert witness for defendants in malpractice cases for Livingston, Barger, Brandt, & Schroeder, LLC ($10,001–$50,000). H.R.P. has served on the advisory board for Ocusciences, Inc. (less than $1,000). T.M.S. does not have a financial relationship with a commercial entity that has an interest in the subject of this manuscript.

Acknowledgments: The authors thank Jeffrey J. Landers for technical assistance with cell-tracking studies.

References

1. Gomez-Mouton C, Lacalle RA, Mira E, Jimenez-Baranda S, Barber DF, Carrera AC, Martinez AC, Manes S. Dynamic redistribution of raft domains as an organizing platform for signaling during cell chemotaxis. *J Cell Biol* 2004;164:759–768.
2. Affolter M, Weijer CJ. Signaling to cytoskeletal dynamics during chemotaxis. *Dev Cell* 2005;9:19–34.
3. Kay RR, Langridge P, Traynor D, Hoeller O. Changing directions in the study of chemotaxis. *Nat Rev Mol Cell Biol* 2008;9:455–463.
4. Nishikimi A, Fukuhara H, Su W, Hongu T, Takasuga S, Mihara H, Cao Q, Sanematsu F, Kanai M, Hasegawa H, *et al.* Sequential regulation of Dock2 dynamics by two phospholipids during neutrophil chemotaxis. *Science* 2009;324:384–387.
5. Pike LJ. Lipid rafts: bringing order to chaos. *J Lipid Res* 2003;44:655–667.
6. Pike LJ. Lipid rafts: heterogeneity on the high seas. *Biochem J* 2004;378:281–292.
7. Cremesti AE, Goni FM, Kolesnick R. Role of sphingomyelinase and ceramide in modulating rafts: do biophysical properties determine biologic outcome? *FEBS Lett* 2002;531:47–53.
8. Ruvolo PP. Intracellular signal transduction pathways activated by ceramide and its metabolites. *Pharmacol Res* 2003;47:383–392.
9. Hannun YA, Obeid LM. Principles of bioactive lipid signalling: lessons from sphingolipids. *Nat Rev Mol Cell Biol* 2008;9:139–150.
10. Pfeiffer A, Bottcher A, Orso E, Kapinsky M, Nagy P, Bodnar A, Spreitzer I, Liebisch G, Drobnik W, Gempel K, *et al.* Lipopolysaccharide and ceramide docking to CD14 provokes ligand-specific receptor clustering in rafts. *Eur J Immunol* 2001;31:3153–3164.
11. Amtmann E, Baader W, Zoller M. Neutral sphingomyelinase inhibitor C11AG prevents lipopolysaccharide-induced macrophage activation. *Drugs Exp Clin Res* 2003;29:5–13.
12. Wong K, Li XB, Hunchuk N. *N*-acetylsphingosine (C2-ceramide) inhibited neutrophil superoxide formation and calcium influx. *J Biol Chem* 1995;270:3056–3062.
13. Feldhaus MJ, Weyrich AS, Zimmerman GA, McIntyre TM. Ceramide generation *in situ* alters leukocyte cytoskeletal organization and beta 2–integrin function and causes complete degranulation. *J Biol Chem* 2002;277:4285–4293.
14. Fuortes M, Jin W, Nathan C. Ceramide selectively inhibits early events in the response of human neutrophils to tumor necrosis factor. *J Leukoc Biol* 1996;59:451–460.
15. Seumois G, Fillet M, Gillet L, Faccinetto C, Desmet C, Francois C, Dewals B, Oury C, Vanderplasschen A, Lekeux P, *et al. De novo* C16- and C24-ceramide generation contributes to spontaneous neutrophil apoptosis. *J Leukoc Biol* 2007;81:1477–1486.
16. Hinkovska-Galcheva V, Kjeldsen L, Mansfield PJ, Boxer LA, Shayman JA, Suchard SJ. Activation of a plasma membrane-associated neutral sphingomyelinase and concomitant ceramide accumulation during IgG-dependent phagocytosis in human polymorphonuclear leukocytes. *Blood* 1998;91:4761–4769.
17. Montes LR, Ruiz-Arguello MB, Goni FM, Alonso A. Membrane restructuring via ceramide results in enhanced solute efflux. *J Biol Chem* 2002;277:11788–11794.
18. Clarke CJ, Hannun YA. Neutral sphingomyelinases and NSMase2: bridging the gaps. *Biochim Biophys Acta* 2006;1758:1893–1901.
19. Mansfield PJ, Hinkovska-Galcheva V, Carey SS, Shayman JA, Boxer LA. Regulation of polymorphonuclear leukocyte degranulation and oxidant production by ceramide through inhibition of phospholipase D. *Blood* 2002;99:1434–1441.
20. Pierini LM, Eddy RJ, Fuortes M, Seveau S, Casulo C, Maxfield FR. Membrane lipid organization is critical for human neutrophil polarization. *J Biol Chem* 2003;278:10831–10841.
21. Heit B, Colarusso P, Kubes P. Fundamentally different roles for LFA-1, MAC-1 and alpha4-integrin in neutrophil chemotaxis. *J Cell Sci* 2005;118:5205–5220.
22. Luberto C, Hassler DF, Signorelli P, Okamoto Y, Sawai H, Boros E, Hazen-Martin DJ, Obeid LM, Hannun YA, Smith GK. Inhibition of tumor necrosis factor-induced cell death in MCF7 by a novel inhibitor of neutral sphingomyelinase. *J Biol Chem* 2002;277:41128–41139.
23. Tani M, Hannun YA. Analysis of membrane topology of neutral sphingomyelinase 2. *FEBS Lett* 2007;581:1323–1328.
24. Xu J, Wang F, Van Keymeulen A, Herzmark P, Straight A, Kelly K, Takuwa Y, Sugimoto N, Mitchison T, Bourne HR. Divergent signals and cytoskeletal assemblies regulate self-organizing polarity in neutrophils. *Cell* 2003;114:201–214.
25. Kindzelskii A, Sitrin R, Petty H. Cutting edge: optical microspectrophotometry supports the existence of gel phase lipid rafts at the lamellipodium of human neutrophils: apparent role in calcium signaling. *J Immunol* 2004;172:4681–4685.
26. Bodin S, Welch MD. Plasma membrane organization is essential for balancing competing pseudopod- and uropod-promoting signals during neutrophil polarization and migration. *Mol Biol Cell* 2005;16:5773–5783.
27. Sitrin RG, Sassanella TM, Landers JJ, Petty HR. Migrating human neutrophils exhibit dynamic spatiotemporal variation in membrane lipid organization. *Am J Respir Cell Mol Biol* 2010;43:498–506.
28. Pestonjamasp KN, Forster C, Sun C, Gardiner EM, Bohl B, Weiner O, Bokoch GM, Glogauer M. Rac1 links leading edge and uropod events through Rho and myosin activation during chemotaxis. *Blood* 2006;108:2814–2820.
29. Zhang H, Sun C, Glogauer M, Bokoch GM. Human neutrophils coordinate chemotaxis by differential activation of Rac1 and Rac2. *J Immunol* 2009;183:2718–2728.
30. Weiner OD, Neilsen PO, Prestwich GD, Kirschner MW, Cantley LC, Bourne HRA. PtdInsp(3)- and Rho GTPase–mediated positive feedback loop regulates neutrophil polarity. *Nat Cell Biol* 2002;4:509–513.
31. Nebl T, Pestonjamasp KN, Leszyk JD, Crowley JL, Oh SW, Luna EJ. Proteomic analysis of a detergent-resistant membrane skeleton from neutrophil plasma membranes. *J Biol Chem* 2002;277:43399–43409.

32. Ciarimboli G. Unraveling the ceramide-calpain-caspase connection in cadmium-induced apoptosis: a novel role for ceramides as activators of calpains: focus on "Cadmium-induced ceramide formation triggers calpain-dependent apoptosis in cultured kidney proximal tubule cells". *Am J Physiol Cell Physiol* 2007;293:C837–C838.
33. Lokuta MA, Nuzzi PA, Huttenlocher A. Calpain regulates neutrophil chemotaxis. *Proc Natl Acad Sci USA* 2003;100:4006–4011.
34. Nuzzi PA, Senetar MA, Huttenlocher A. Asymmetric localization of calpain 2 during neutrophil chemotaxis. *Mol Biol Cell* 2007;18:795–805.
35. Suchard SJ, Mansfield PJ, Boxer LA, Shayman JA. Mitogen-activated protein kinase activation during IgG-dependent phagocytosis in human neutrophils: inhibition by ceramide. *J Immunol* 1997;158:4961–4967.
36. Iwabuchi K, Prinetti A, Sonnino S, Mauri L, Kobayashi T, Ishii K, Kaga N, Murayama K, Kurihara H, Nakayama H, *et al.* Involvement of very long fatty acid–containing lactosylceramide in lactosylceramide-mediated superoxide generation and migration in neutrophils. *Glycoconj J* 2008;25:357–374.
37. Mansfield PJ, Carey SS, Hinkovska-Galcheva V, Shayman JA, Boxer LA. Ceramide inhibition of phospholipase D and its relationship to RhoA and ARF1 translocation in GTP gamma S–stimulated polymorphonuclear leukocytes. *Blood* 2004;103:2363–2368.
38. Chiba N, Masuda A, Yoshikai Y, Matsuguchi T. Ceramide inhibits LPS-induced production of IL-5, IL-10, and IL-13 from mast cells. *J Cell Physiol* 2007;213:126–136.
39. Suchard SJ, Hinkovska-Galcheva V, Mansfield PJ, Boxer LA, Shayman JA. Ceramide inhibits IgG-dependent phagocytosis in human polymorphonuclear leukocytes. *Blood* 1997;89:2139–2147.
40. Heit B, Tavener S, Raharjo E, Kubes P. An intracellular signaling hierarchy determines direction of migration in opposing chemotactic gradients. *J Cell Biol* 2002;159:91–102.
41. Heit B, Robbins SM, Downey CM, Guan Z, Colarusso P, Miller BJ, Jirik FR, Kubes P. PTEN functions to "prioritize" chemotactic cues and prevent "distraction" in migrating neutrophils. *Nat Immunol* 2008;9:743–752.
42. Merrill AH Jr, Schmelz EM, Dillehay DL, Spiegel S, Shayman JA, Schroeder JJ, Riley RT, Voss KA, Wang E. Sphingolipids—the enigmatic lipid class: biochemistry, physiology, and pathophysiology. *Toxicol Appl Pharmacol* 1997;142:208–225.
43. Spiegel S. Sphingosine 1–phosphate: a ligand for the Edg-1 family of G-protein–coupled receptors. *Ann N Y Acad Sci* 2000;905:54–60.
44. Rahaman M, Costello RW, Belmonte KE, Gendy SS, Walsh MT. Neutrophil sphingosine 1–phosphate and lysophosphatidic acid receptors in pneumonia. *Am J Respir Cell Mol Biol* 2006;34:233–241.
45. Kee TH, Vit P, Melendez AJ. Sphingosine kinase signalling in immune cells. *Clin Exp Pharmacol Physiol* 2005;32:153–161.
46. Tepper AD, Diks SH, van Blitterswijk WJ, Borst J. Glucosylceramide synthase does not attenuate the ceramide pool accumulating during apoptosis induced by CD95 or anti-cancer regimens. *J Biol Chem* 2000;275:34810–34817.
47. Contreras FX, Villar AV, Alonso A, Kolesnick RN, Goni FM. Sphingomyelinase activity causes transbilayer lipid translocation in model and cell membranes. *J Biol Chem* 2003;278:37169–37174.
48. Tepper AD, Ruurs P, Wiedmer T, Sims PJ, Borst J, van Blitterswijk WJ. Sphingomyelin hydrolysis to ceramide during the execution phase of apoptosis results from phospholipid scrambling and alters cell-surface morphology. *J Cell Biol* 2000;150:155–164.
49. Jandak J, Li XL, Kessimian N, Steiner M. Unequal distribution of membrane components between pseudopodia and cell bodies of platelets. *Biochim Biophys Acta* 1990;1029:117–126.